

## 불연속 변화단면 수평 곡선보의 자유진동

### Free Vibrations of Stepped Horizontally Curved Beams

이 병 구\* · 진 태 기\*\* · 김 선 기\*\* · 신 성 철\*\*

Byoung Koo Lee · Tae Ki Jin · Sun Ki Kim · Sung Chul Shin

---

#### Abstract

The differential equations governing the free vibrations of stepped horizontally circular curved beams with circular cross-section are derived and solved numerically. In numerical method, the Runge-Kutta and Determinant Search methods are used for computing the natural frequencies and mode shapes. Frequencies and mode shapes are reported as the functions of non-dimensional system parameters. The numerical method developed herein for computing frequencies and mode shapes are efficient and reliable.

*Keywords: curved beam, free vibration, natural frequency, mode shape, stepped beam*

---

#### 1. INTRODUCTION

Studies on the free vibrations of linearly elastic curved beams of various geometries have been reported by many investigators.<sup>(1) (4)</sup> However, the works on the free vibration of horizontally curved beam with variable cross-section, especially stepped curved beams, are very rare. The main purpose of the present paper is, therefore, to present numerical method for calculating the natural frequencies and mode shapes of stepped horizontally curved beams.

The differential equations were derived for free, out-of-plane vibration of linearly elastic circular curved beam with variable cross-section, and the stepped curved beam with circular cross-section was applied into this differential equations. The governing differential equations were solved numerically to obtain the natural frequencies and mode shapes. In numerical method, the Runge-Kutta and the Determinant Search methods were used to integrate the differential equations and calculate the natural frequencies, respectively. In numerical examples, the curved beams with both clamped ends and both hinged ends were considered. The four lowest natural frequencies were presented as functions of the non-dimensional system parameters.

---

\* Member · Professor, Dept. of Civil Engineering, Wonkwang University

\*\* Graduate Student, Dept. of Civil Engineering, Wonkwang University

## 2. MATHEMATICAL MODEL

The geometry of stepped horizontally circular curved beam is defined in Figure 1. Both ends are either clamped or hinged. Its radius and opening angle are  $a$  and  $\alpha$ , respectively. The radial line to a typical beam point is inclined at angle  $\theta$  with the radial line of left end. Also shown in Figure 1 are positive direction of vertical displacement  $v$ , positive directions of rotation  $\psi$  and  $\beta$  of cross-section due to the bending moment and shear force, respectively, and positive direction of angle of twist  $\phi$ . The beam is sectored into several segments for the stepped cross-section. The segment ratio which is defined as a ratio of the subtended angle of  $i$ th segment to the opening angle  $\alpha$  is depicted as  $m_i$ . The thickness, cross-sectional area, area moment of inertia and torsional constant of cross-section of the  $i$ th segment are  $D_i$ ,  $A_i$ ,  $I_i$  and  $J_i$  ( $i=1, 2, 3, \dots, n$ ), respectively.

The quantities  $A_i$ ,  $I_i$  and  $J_i$  of the  $i$ th segment are expressed in the form

$$A_i = A_1 f_i, \quad I_i = I_1 g_i, \quad J_i = J_1 h_i \quad (1-3)$$

where  $f_i = f(\theta)$ ,  $g_i = g(\theta)$  and  $h_i = h(\theta)$  are the functions of the single variable  $\theta$  in the  $i$ th segment as discussed later in shape functions of the section 3.

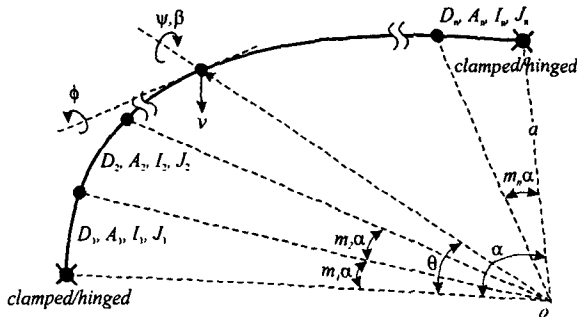


Fig. 1 Geometry of curved beam

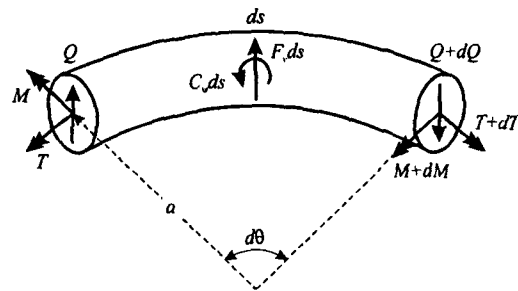


Fig. 2 Loads on a curved beam element

A small element of the curved beam with the opening angle  $d\theta$  and arc length  $ds$  shown in Figure 2 defines the positive directions for the shear force  $Q$ , the bending moment  $M$ , the torsional moment  $T$ , the vertical inertia force  $F_v$  and the rotatory inertia couple  $C_\phi$ . With the inertia force and the rotatory inertia couple treated as equivalent static quantities, the three equations for dynamic equilibrium of element are

$$\frac{dQ}{d\theta} - aF_v = 0, \quad \frac{dM}{d\theta} - aQ + T + aC_\phi = 0, \quad M - \frac{dT}{d\theta} = 0 \quad (4-6)$$

The equations that relate  $M$  and  $T$  to the rotations  $\psi$  and  $\phi$  are as follows.<sup>(5)</sup>

$$M = \frac{EI}{a} \left( \phi - \frac{d\psi}{d\theta} \right) = \frac{EI_1 g}{a} \left( \phi - \frac{d\psi}{d\theta} \right), \quad T = \frac{GI}{a} \left( \psi + \frac{d\phi}{d\theta} \right) = \frac{GJ_1 h}{a} \left( \psi + \frac{d\phi}{d\theta} \right) \quad (7-8)$$

where  $E$  and  $G$  are the Young's modulus and shear modulus, respectively.

The transverse shear force  $Q$ , whose effect on the structural behavior is known as the effect of shear deformation, is given by<sup>(6)</sup>

$$Q = k\beta GA = kGA_1 f \left( \frac{1}{a} \frac{dv}{d\theta} - \psi \right) \quad (9)$$

where  $k$  is the cross-sectional shape factor. For example, the  $k$  values for the rectangular and circular sections are 2/3 and 3/4, respectively.

The beam is assumed to be in harmonic motion, or each co-ordinate is proportional to  $\sin(\omega t)$  where  $\omega$  is the frequency parameter and  $t$  is time. The inertia loadings per unit arc length are then

$$F_v = -dA\omega^2 v = -dA_1 f \omega^2 v, \quad C_\psi = -dIa\omega^2 \psi = -dI_1 g a \omega^2 \psi \quad (10,11)$$

where  $d$  is mass density of beam material. The  $C_\psi$  term of equation (11) is known as the effect of rotatory inertia in free vibrations.

To facilitate the numerical studies, the following non-dimensional system parameters are defined.

$$\eta = v/a, \quad \lambda = \frac{a}{\sqrt{I_1/A_1}}, \quad \gamma = kG/E, \quad \epsilon = GJ_1/(EI_1), \quad p_i = \omega_i a^2 \sqrt{dA_1/(EI_1)} \quad (12-16)$$

The vertical displacement  $v$  is normalized by the curved beam radius  $a$  and the variables of  $\lambda$ ,  $\gamma$ ,  $\epsilon$  and  $p_i$  are the slenderness ratio, shear parameter, stiffness parameter and frequency parameter, respectively.

When equations (9) and (10) are substituted into equation (4) and the non-dimensional forms of equations (12)-(16) are used, the result is

$$\frac{d^2 \eta}{d\theta^2} = -\frac{1}{f} \frac{df}{d\theta} \frac{d\eta}{d\theta} - \frac{p_i^2}{\gamma \lambda^2} \eta + \frac{d\psi}{d\theta} + \frac{1}{f} \frac{df}{d\theta} \psi \quad (17)$$

When equations (7), (8), (9) and (11) are substituted into equation (5) and the non-dimensional forms of equations (12)-(16) are used, the result is

$$\begin{aligned} \frac{d^2\psi}{d\theta^2} = & -\gamma\lambda^2 \frac{f}{g} \frac{d\eta}{d\theta} - \frac{1}{g} \frac{dg}{d\theta} \frac{d\psi}{d\theta} + \left( \gamma\lambda^2 \frac{f}{g} + \varepsilon \frac{h}{g} - \frac{p_i^2}{\lambda^2} \right) \psi \\ & + \left( 1 + \varepsilon \frac{h}{g} \right) \frac{d\phi}{d\theta} + \frac{1}{g} \frac{dg}{d\theta} \phi \end{aligned} \quad (18)$$

When equations (7) and (8) are substituted into equation (6) and the non-dimensional forms of equations (12)-(16) are used, the result is

$$\frac{d^2\phi}{d\theta^2} = - \left( 1 + \frac{g}{\varepsilon h} \right) \frac{d\psi}{d\theta} - \frac{1}{h} \frac{dh}{d\theta} \left( \psi + \frac{d\phi}{d\theta} \right) + \frac{1}{\varepsilon} \frac{g}{h} \phi \quad (19)$$

For the beam with both clamped ends, the boundary conditions at ends  $\theta=0$  and  $\theta=a$  are

$$\eta=0, \quad d\eta/d\theta=0, \quad \phi=0 \quad (20-22)$$

For the beam with both hinged ends, the boundary conditions at ends  $\theta=0$  and  $\theta=a$  are

$$\eta=0, \quad d\psi/d\theta=0, \quad \phi=0 \quad (23-25)$$

### 3. SHAPE FUNCTIONS: $f$ , $g$ and $h$

The shape functions  $f$ ,  $g$  and  $h$  first introduced in equations (1), (2) and (3), and contained in the governing differential equations (17), (18) and (19), are now defined. The examples are limited circular cross-section whose diameter of  $i$ th segment is  $D_i$  mentioned above already. A non-dimensional system parameter defined as the section ratio is introduced newly as follows.

$$n_i = D_i/D_1 \quad (26)$$

in which it is clear that the value of  $n_1$  is one because of  $n_1 = D_1/D_1 = 1$ .

With equations (1), (2), (3) and (26), the  $f_i$ ,  $g_i$  and  $h_i$  of the circular cross-section for the  $i$ th segment are expressed in term of section ratio  $n_i$  as follows.

$$f_i = n_i^2, \quad g_i = h_i = n_i^4 \quad (27,28)$$

When equations (27) and (28) are differentiated once, the results are

$$df/d\theta=0, \quad dg/d\theta=0, \quad dh/d\theta=0 \quad (29)$$

#### 4. NUMERICAL METHOD AND COMPUTED RESULTS

Based on the above analysis, a general FORTRAN computer program was written to calculate  $p_i$ ,  $\eta = \eta_i(\theta)$ ,  $\psi = \psi_i(\theta)$  and  $\phi = \phi_i(\theta)$ . The numerical method described by Oh et al.<sup>(7)</sup> was used to solve the differential equations (17)-(19), subjected to the end constraint equations (20)-(22) or (23)-(25). The curved beams with both clamped ends and both hinged ends were considered for given parameters  $\alpha$ ,  $m_i$ ,  $n_i$ ,  $\lambda$ ,  $\gamma$  and  $\epsilon$ . First, the Runge-Kutta method was used to integrate the differential equations; and then the Determinant Search method was used to calculate the characteristic values  $p_i$ .

In this study, the shear parameter  $\gamma$  and stiffness parameter  $\epsilon$  were chosen as 0.29 and 0.77, respectively, since the cross-section was circular with  $k=3/4$  and  $J_1=2I_1$ , and the material was assumed to be steel with  $G/E=0.385$ . The four lowest values of  $p_i$  with their corresponding mode shapes were calculated.

For numerical examples, suitable convergence of solutions was obtained for an increment of  $\Delta\theta = \alpha/50$  in Runge-Kutta method. The convergence criterion was that  $p_i$  solutions obtained with the  $\alpha/50$  increment agreed with those obtained with the  $\alpha/300$  increment to within three significant figures. The numerical results, given in Table 1 and Figures 3-7, are summarized as follows.

For the comparison purposes, the finite element solutions based on the commercial package SAP 90 were used to compute the frequency parameters  $p_i$ . The results are shown in Table 1 in which the frequencies of this study agree closely with those of SAP 90 within a tolerance of 3%.

Table 1 Comparison of frequency parameters  $p_i$  between this study and SAP 90  
( $\alpha = 60^\circ$ ,  $m_1 = m_2 = m_3 = 0.33$ ,  $n_2 = 1.2$ ,  $n_3 = 1$ ,  $\lambda = 80$ ,  $\gamma = 0.29$ ,  $\epsilon = 0.77$ )

End constraints	$i$	Frequency parameter, $p_i$		Deviation (%)  B-A /A
		this study(A)	SAP 90(B)	
both clamped ends	1	19.89	20.09	1.01
	2	58.32	59.97	2.83
	3	112.1	110.4	1.52
	4	179.5	180.9	0.78
both hinged ends	1	7.528	7.589	0.81
	2	36.98	36.26	1.94
	3	81.34	82.18	1.03
	4	142.2	141.2	0.70

It is shown in Figure 3, for which both clamped ends and both hinged ends with  $\alpha = 60^\circ$ ,  $m_1 = m_2 = m_3 = 0.33$ ,  $n_3 = 1$ ,  $\lambda = 80$ ,  $\gamma = 0.29$ ,  $\epsilon = 0.77$  that the frequency parameters  $p_i$  increase as the section ratio  $n_2$  increases to 3. It is observed that the increasing rate of  $p_i$  vs.  $n_2$  curves is higher at higher mode. Particularly, the increasing rate of first mode is negligible.

It is shown in Figure 4, for which both clamped ends and both hinged ends with  $\alpha = 60^\circ$ ,  $m_1 = m_3 = (1 - m_2)/2$ ,  $n_2 = 1.2$ ,  $n_3 = 1$ ,  $\lambda = 80$ ,  $\gamma = 0.29$ ,  $\epsilon = 0.77$ , that the  $p_i$  values increase as the segment ratio  $m_2$  increases. It is noted that in case of the first mode of the both hinged ends, the effect of  $m_2$  on  $p_i$  is negligible.

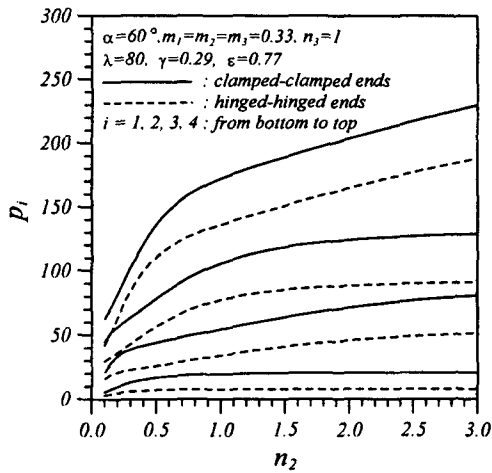


Fig. 3  $p_i$  vs.  $n_2$  curves

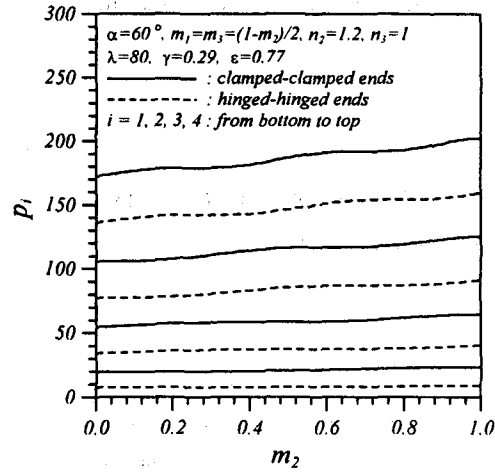


Fig. 4  $p_i$  vs.  $m_2$  curves

It is shown in Figure 5, for which both clamped and both hinged beams with  $\alpha = 60^\circ$ ,  $m_1 = m_2 = m_3 = 0.33$ ,  $n_2 = 1.2$ ,  $n_3 = 1$ ,  $\gamma = 0.29$ ,  $\epsilon = 0.77$ , that the  $p_i$  values increase and approach upper limits or horizontal asymptotes as the slenderness ratio  $\lambda$  increases to 200. It is noted that in case of the first modes, the effect of  $\lambda$  on  $p_i$  is negligible.

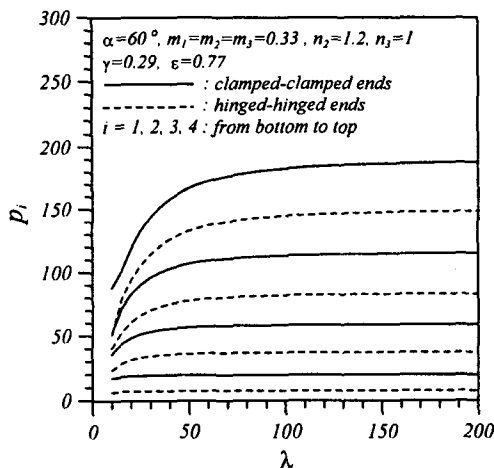


Fig. 5  $p_i$  vs.  $\lambda$  curves

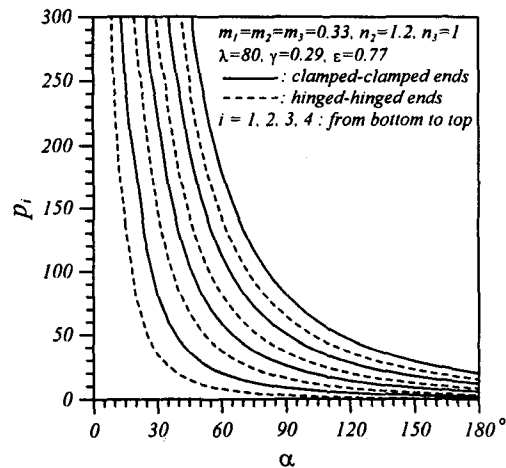


Fig. 6  $p_i$  vs.  $\alpha$  curves

In Figure 6, both clamped ends, both hinged ends,  $m_1 = m_2 = m_3 = 0.33$ ,  $n_2 = 1.2$ ,  $n_3 = 1$ ,  $\lambda = 80$ ,  $\gamma = 0.29$ ,  $\varepsilon = 0.77$  and the  $p_i$  values all decrease very rapidly as the opening angle  $\alpha$  increases from  $30^\circ$  to  $90^\circ$ . And it is true that the  $p_i$  values approach lower limits or horizontal asymptotes as  $\alpha$  increases to  $180^\circ$ .

Typical mode shapes are shown in Figure 7, based on both clamped ends and both hinged ends,  $m_1 = m_2 = m_3 = 0.33$ ,  $n_2 = 1.2$ ,  $n_3 = 1$ ,  $\lambda = 80$ ,  $\gamma = 0.29$ ,  $\varepsilon = 0.77$ ,  $\alpha = 60^\circ$ .

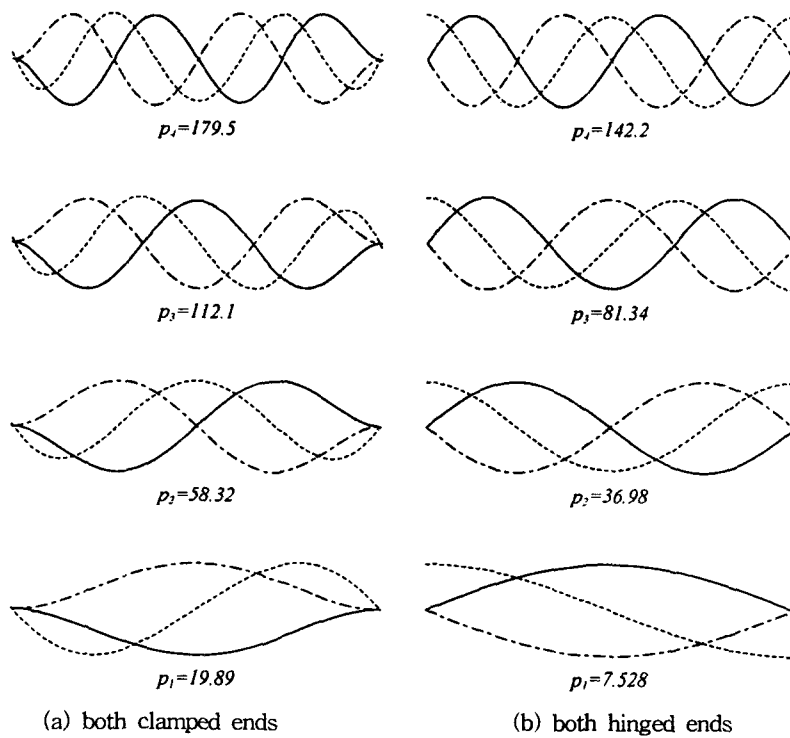


Fig. 7 Example of mode shapes ( $\alpha = 60^\circ$ ,  $m_1 = m_2 = m_3 = 0.33$ ,  $n_2 = 1.2$ ,  $n_3 = 1$ ,  $\lambda = 80$ ,  $\gamma = 0.29$ ,  $\varepsilon = 0.77$ ; — :  $v$ , - - - :  $\psi$ , - · - · :  $\phi$ )

## 6. CONCLUSIONS

The method presented here for calculating frequencies and mode shapes for stepped horizontally circular curved beams were found to be efficient and reliable over a wide range of system parameters. Governing differential equations for free vibration of such curved beam were derived and solved numerically. Computations showed that the frequencies obtained by present study and SAP 90 agreed closely. The lowest four frequency parameters are presented as functions of four non-dimensional system parameters.

## ACKNOWLEDGEMENT

This work was supported by Grant No. 2000-1-31100-006-1 from the Basic Research Program of the Korea Science & Engineering Foundation. The authors thank for this financial support.

## REFERENCES

1. Yonezawa, H, "Moments and Free Vibrations in Curved Girder Bridges," *Journal of the Engineering Mechanics Division, ASCE*, No. EM1, 1962, pp.1-22.
2. Tan, C.P. and Shore, S., "Dynamic Response of a Horizontally Curved Bridge," *Journal of the Structural Division, ASCE*, Vol. 94, No. ST3, 1968, pp.761-781.
3. Wang, T.M. and Lee, J.M., "Natural Frequencies of Multi-span Circular Curved Frames," *International Journal of Solids and Structures*, Vol. 8, 1972, pp.791-805.
4. Wang, T.M., Nettleton, R.H. and Keita, B., "Natural Frequencies for Out of Plane Vibrations of Continuous Curved Beams," *Journal of Sound and Vibration*, Vol. 68, No. 3, 1980, pp.427-436.
5. Volterra, E. and Gaines, J.H., *Advanced Strength of Materials*, Prentice-Hall Inc., 1971.
6. Gere, J.M. and Timoshenko, S.P., *Mechanics of Materials*, 2nd Edition, Brooks/Cole Engineering Division, 1984.
7. Oh, S.J., Lee, B.K. and Lee, I.W., "Free Vibrations of Non-circular Arches with Non-uniform Cross-section," *Journal of Solids and Structures*, Vol. 37, No. 36, 2000, pp.4871-4891.
8. Carnahan, B., Luther, H.A. and Wilkes, J.O., *Applied Numerical Methods*, John Wiley & Sons, 1969.